Chapter 9

Qualitative dynamics, for pedestrians

In this chapter we begin to learn how to use qualitative properties of a flow in order to *partition* the phase space in a topologically invariant way, and *name* topologically distinct orbits. This will enable us (in the next chapter) to *count* the distinct orbits, and in the process touch upon all the main themes of this book, going the whole distance from diagnosing chaotic dynamics to computing zeta functions.

We start by a simple physical example, symbolic dynamics of a 3-disk game of pinball, and then show that also for smooth flows the qualitative dynamics of stretching and folding flows enables us to partition the phase space and assign symbolic dynamics itineraries to trajectories. Here we illustrate the method on a $1-d$ approximation to Rössler flow. We then turn this topological dynamics into a multiplicative operation on the phase space partition by means of transition matrices/Markov graphs.

Even though by inclination you might only care about the serious stuff, like Rydberg atoms or mesoscopic devices, and resent wasting time on things formal, this chapter and the next are good for you. Read them.

9.1 Itineraries

(R. Mainieri and P. Cvitanović)

What can a flow do to the phase space points? This is a very difficult question to answer because we have assumed very little about the evolution function f^t; continuity, and differentiability a sufficient number of times.

Trying to make sense of this question is one of the basic concerns in the study of dynamical systems. One of the first answers was inspired by the motion of the planets: they appear to repeat their motion through the firmament. Motivated by this observation, the first attempts to describe dynamical systems were to think of them as periodic.

However, periodicity is almost never quite exact. What one tends to observe is recurrence. A recurrence of a point x_0 of a dynamical system is a return of that point to a neighborhood of where it started. How close the point x_0 must return is up to us: we can choose a volume of any size and shape as long as it encloses x_0, and call it the neighborhood $\mathcal{M}_0$. For chaotic dynamical systems, the evolution might bring the point back to the starting neighborhood infinitely often. That is, the set

$$\{y \in \mathcal{M}_0 : \quad y = f^t(x_0), \quad t > t_0\} \tag{9.1}$$

will in general have an infinity of recurrent episodes.

To observe a recurrence we must look at neighborhoods of points. This suggests another way of describing how points move in phase space, which turns out to be the important first step on the way to a theory of dynamical systems: qualitative, topological dynamics, or, as it is usually called, *symbolic dynamics*. As the subject can get quite technical, a summary of the basic notions and definitions of symbolic dynamics is relegated to sect. 9.7; check that section whenever you run into obscure symbolic dynamics jargon.

We start by cutting up the phase space up into regions $\mathcal{M}_A, \mathcal{M}_B, \ldots, \mathcal{M}_Z$. This can be done in many ways, not all equally clever. Any such division of the phase space into topologically distinct regions is a *partition*, and we associate with each region (sometimes referred to as a *state*) a symbol s from an N-letter *alphabet* or *state set* $\mathcal{A} = \{A, B, C, \cdots, Z\}$. As the dynamics moves the point through the phase space, different regions will be visited. The visitation sequence - forthwith referred to as the *itinerary* - can be represented by the letters of the alphabet $\mathcal{A}$. If, as in the example sketched in fig. 9.1, the phase space is divided into three regions $\mathcal{M}_0$, $\mathcal{M}_1$, and $\mathcal{M}_2$, the "letters" are the integers $\{0, 1, 2\}$, and the itinerary for the trajectory sketched in the figure is $0 \mapsto 2 \mapsto 1 \mapsto 0 \mapsto 1 \mapsto 2 \mapsto \cdots$.

If there is no way to reach partition $\mathcal{M}_i$ from partition $\mathcal{M}_j$, and conversely, partition $\mathcal{M}_j$ from partition $\mathcal{M}_i$, the phase space consists of at least two disconnected pieces, and we can analyze it piece by piece. An interesting partition should be dynamically connected, that is one should be able to go from any region $\mathcal{M}_i$ to any other region $\mathcal{M}_j$ in a finite number of steps. A dynamical system with such partition is said to be *metrically indecomposable*.

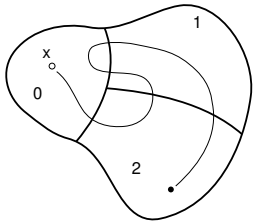

Figure 9.1: A trajectory with itinerary 021012.

In general one also encounters transient regions - regions to which the dynamics does not return to once they are exited. Hence we have to distinguish between (for us uninteresting) wandering trajectories that never return to the initial neighborhood, and the non–wandering set (2.2) of the *recurrent* trajectories.

The allowed transitions between the regions of a partition are encoded in the $[N\times N]$-dimensional *transition matrix* whose elements take values

$$T_{ij} = \begin{cases} 1 & \text{if a transition region } \mathcal{M}_j \to \text{region } \mathcal{M}_i \text{ is possible} \\ 0 & \text{otherwise}. \end{cases} \tag{9.2}$$

An example is the complete N-ary dynamics for which all transition matrix entries equal unity (one can reach any region from any other region in one step)

$$T_c = \begin{pmatrix} 1 & 1 & \dots & 1 \\ 1 & 1 & \dots & 1 \\ \vdots & \vdots & \ddots & \vdots \\ 1 & 1 & \dots & 1 \end{pmatrix}. \tag{9.3}$$

Further examples of transition matrices, such as the 3-disk transition matrix (9.5) and the 1-step memory sparse matrix (9.14), are peppered throughout the text. The transition matrix encodes the topological dynamics as an invariant law of motion, with the allowed transitions at any instant independent of the trajectory history, requiring no memory.

Knowing that a point from $\mathcal{M}_i$ reaches $\mathcal{M}_j$ in one step is not quite good enough. We would be happier if we knew that *any* point in $\mathcal{M}_i$ reaches $\mathcal{M}_j$; otherwise we have to subpartition $\mathcal{M}_i$ into the points which land in $\mathcal{M}_j$, and those which do not, and often we will find ourselves partitioning *ad infinitum*.

Such considerations motivate the notion of a *Markov partition*, a partition for which no memory of preceding steps is required to fix the transitions

1.1
page 32

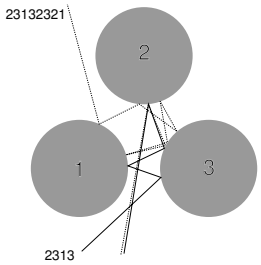

Figure 9.2: Two pinballs that start out very close to each other exhibit the same qualitative dynamics _2313_ for the first three bounces, but due to the exponentially growing separation of trajectories with time, follow different itineraries thereafter: one escapes after _2313_, the other one escapes after _23132321_.

allowed in the next step. Dynamically, *finite Markov partitions* can be generated by *expanding* d-dimensional iterated mappings $f : \mathcal{M} \to \mathcal{M}$, if $\mathcal{M}$ can be divided into N regions $\{\mathcal{M}_0, \mathcal{M}_1, \dots, \mathcal{M}_{N-1}\}$ such that in one step points from an initial region $\mathcal{M}_i$ either fully cover a region $\mathcal{M}_j$, or miss it altogether,

$$\text{either} \quad \mathcal{M}_j \cap f(\mathcal{M}_i) = \emptyset \quad \text{or} \quad \mathcal{M}_j \subset f(\mathcal{M}_i)\,. \tag{9.4}$$

An example is the 1-dimensional expanding mapping sketched in fig. 9.8, and more examples are worked out in sect. 20.2.

Example 9.1 3-disk symbolic dynamics

The key symbolic dynamics concepts are easily illustrated by a game of pinball. Consider the motion of a free point particle in a plane with N elastically reflecting convex disks. After a collision with a disk a particle either continues to another disk or escapes, and any trajectory can be labelled by the disk sequence. For example, if we label the three disks by 1, 2 and 3, the two trajectories in fig. 9.2 have itineraries _2313_, _23132321_ respectively. The 3-disk prime cycles given in figs. 1.5 and 9.5 are further examples of such itineraries.

At each bounce a cone of initially nearby trajectories defocuses (see fig. 1.7), and in order to attain a desired longer and longer itinerary of bounces the initial point $x_0 = (s_0, p_0)$ has to be specified with a larger and larger precision, and lie within initial phase space strips drawn in fig. 9.3. Similarly, it is intuitively clear that as we go backward in time (in this case, simply reverse the velocity vector), we also need increasingly precise specification of $x_0 = (s_0, p_0)$ in order to follow a given past itinerary. Another way to look at the survivors after two bounces is to plot $\mathcal{M}_{s_1.s_2}$, the intersection of $\mathcal{M}_{.s_2}$ with the strips $\mathcal{M}_{s_1.}$ obtained by time reversal (the velocity changes sign $\sin\phi \to -\sin\phi$). $\mathcal{M}_{s_1.s_2}$ is a "rectangle" of nearby trajectories which have arrived from the disk s_1 and are heading for the disk s_2.

We see that a finite length trajectory is not uniquely specified by its finite itinerary, but an isolated unstable cycle (consisting of infinitely many repetitions of a prime building block) is. More generally, for hyperbolic flows the intersection of the future and past itineraries, the bi-infinite itinerary $S^-.S^+ = \cdots s_{-2}s_{-1}s_0.s_1s_2s_3\cdots$ specifies a unique trajectory. This is intuitively clear for our 3-disk game of pinball,

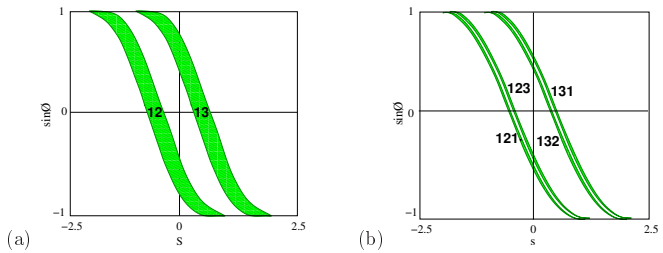

Figure 9.3: The 3-disk game of pinball Poincaré section, trajectories emanating from the disk 1 with x_0 = (arclength, parallel momentum) = (s_0, p_0) , disk radius : center separation ratio a:R = 1:2.5. (a) Strips of initial points $\mathcal{M}_{12}$, $\mathcal{M}_{13}$ which reach disks 2, 3 in one bounce, respectively. (b) Strips of initial points $\mathcal{M}_{121}$, $\mathcal{M}_{131}$ $\mathcal{M}_{132}$ and $\mathcal{M}_{123}$ which reach disks 1, 2, 3 in two bounces, respectively. (Y. Lan)

and is stated more formally in the definition (9.4) of a Markov partition. The definition requires that the dynamics be expanding forward in time in order to ensure that the cone of trajectories with a given itinerary becomes sharper and sharper as the number of specified symbols is increased.

As the disks are convex, there can be no two consecutive reflections off the same disk, hence the covering symbolic dynamics consists of all sequences which include no symbol repetitions _11_, _22_, _33_. *This is a finite set of finite length* pruning rules, *hence, the dynamics is a subshift of finite type, with the transition matrix (9.2) given by*

$$T = \begin{pmatrix} 0 & 1 & 1 \\ 1 & 0 & 1 \\ 1 & 1 & 0 \end{pmatrix} . \qquad (9.5)$$

For convex disks the separation between nearby trajectories increases at every reflection, implying that the stability matrix has an expanding eigenvalue. By the Liouville phase-space volume conservation (5.10), the other transverse eigenvalue is contracting. This example demonstrates that finite Markov partitions can be constructed for hyperbolic *dynamical systems which are expanding in some directions, contracting in others.*

Determining whether the symbolic dynamics is complete (as is the case for sufficiently separated disks), pruned (for example, for touching or overlapping disks), or only a first coarse graining of the topology (as, for example, for smooth potentials with islands of stability) requires case-by-case investigation. For the time being we assume that the disks are sufficiently separated that there is no additional pruning beyond the prohibition of self-bounces.

9.1
page 169

fast track:
sect. 9.2, p. 153

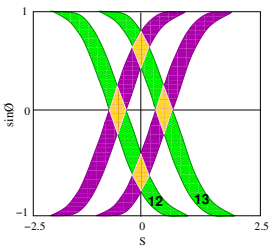

Figure 9.4: The Poincaré section of the phase space for the binary labelled pinball, see also fig. 9.5(b). For definitiveness, this set is generated by starting from disk 1, preceded by disk 2. Indicated are the fixed points $\overline{0}$, $\overline{1}$ and the 2-cycle periodic points $\overline{01}$, $\overline{10}$, together with strips which survive 1, 2, ...bounces. Iteration corresponds to the decimal point shift; for example, all points in the rectangle [01.01] map into the rectangle [010.1] in one iteration.
PC: do this figure right, in terms of strips!

9.1.1 A brief detour; recoding, symmetries, tilings

Though a useful tool, Markov partitioning is not without drawbacks. One glaring shortcoming is that Markov partitions are not unique: any of many different partitions might do the job. The 3-disk system offers a simple illustration of different Markov partitioning strategies for the same dynamical system.

The $\mathcal{A} = \{1, 2, 3\}$ symbolic dynamics for 3-disk system is neither unique, nor necessarily the smartest one - before proceeding it pays to exploit the symmetries of the pinball in order to obtain a more efficient description. As we shall see in chapter 19, rewards of this desymmetrization will be handsome.

As the three disks are equidistantly spaced, our game of pinball has a sixfold symmetry. For instance, the cycles $\overline{12}$, $\overline{23}$, and $\overline{13}$ are related to each other by rotation by $\pm 2\pi/3$ or, equivalently, by a relabelling of the disks. Further examples of such symmetries are shown in fig. 1.5. We note that the disk labels are arbitrary; what is important is how a trajectory evolves as it hits subsequent disks, not what label the starting disk had. We exploit this symmetry by *recoding*, in this case replacing the absolute disk labels by relative symbols, indicating the type of the collision. For the 3-disk game of pinball there are two topologically distinct kinds of collisions, fig. 1.4:

$$\begin{aligned} 0 &: \text{ pinball returns to the disk it came from} \\ 1 &: \text{ pinball continues to the third disk .} \end{aligned} \qquad (9.6)$$

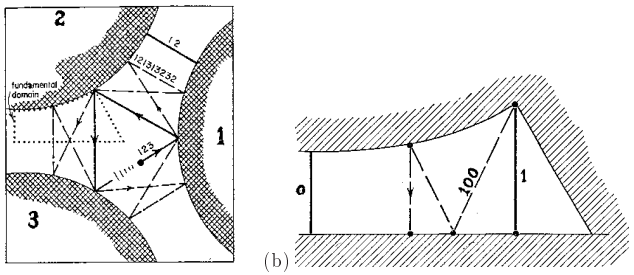

Figure 9.5: The 3-disk game of pinball with the disk radius : center separation ratio a:R = 1:2.5. (a) The three disks, with $\overline{12}$, $\overline{123}$ and $\overline{12123213}$ cycles indicated. (b) The fundamental domain, that is the small 1/6th wedge indicated in (a), consisting of a section of a disk, two segments of symmetry axes acting as straight mirror walls, and an escape gap. The above cycles restricted to the fundamental domain are now the two fixed points $\overline{0}$, $\overline{1}$, and the $\overline{100}$ cycle.

9.2 page 169

This *binary* symbolic dynamics has two immediate advantages over the ternary one; the prohibition of self-bounces is automatic, and the coding utilizes the symmetry of the 3-disk pinball game in elegant manner. If the disks are sufficiently far apart there are no further restrictions on symbols, the symbolic dynamics is complete, and *all* binary sequences are admissible itineraries. As this type of symbolic dynamics pops up frequently, we list the shortest binary prime cycles in table 9.2.

9.3 page 169

Given a ternary sequence and labels of 2 preceding disks these rules fix the corresponding binary symbol. For example

ternary:	3	1	2	1	3	1	2	3	2	1	2	3	1	3	2	3
binary:		.	0	1	0	1	1	0	1	0	1	1	0	1	0	0

(9.7)

The first 2 disks initialize the trajectory and its direction. Due to the 3-disk symmetry the six 3-disk sequences initialized by 12, 13, 21, 23, 31, 32 respectively have the same weights, the same size partitions, and are coded by a single binary sequence. For periodic orbits, the equivalent ternary cycles reduce to binary cycles of 1/3, 1/2 or the same length. How this works is best understood by inspection of table 9.1, fig. 9.5 and fig. 19.3.

The 3-disk game of pinball is tiled by six copies of the *fundamental domain*, a one-sixth slice of the full 3-disk system, with the symmetry axes acting as reflecting mirrors, see fig. 9.5b. A global 3-disk trajectory maps into its fundamental domain mirror trajectory by replacing every crossing of a symmetry axis by a reflection. Depending on the symmetry of the global

$\bar{p}$	p	$\mathbf{g}_{\bar{p}}$
0	1 2	σ_{12}
1	1 2 3	C_3
01	12 13	σ_{23}
001	121 232 313	C_3
011	121 323	σ_{13}
0001	1212 1313	σ_{23}
0011	1212 3131 2323	C_3^2
0111	1213 2123	σ_{12}
00001	12121 23232 31313	C_3
00011	12121 32323	σ_{13}
00101	12123 21213	σ_{12}
00111	12123	e
01011	12131 23212 31323	C_3
01111	12132 13123	σ_{23}

$\bar{p}$	p	$\mathbf{g}_{\bar{p}}$
000001	121212 131313	σ_{23}
000011	121212 313131 232323	C_3^2
000101	121213	e
000111	121213 212123	σ_{12}
001011	121232 131323	σ_{23}
001101	121231 323213	σ_{13}
001111	121231 232312 313123	C_3
010111	121312 313231 232123	C_3^2
011111	121321 323123	σ_{13}
0000001	1212121 2323232 3131313	C_3
0000011	1212121 3232323	σ_{13}
0000101	1212123 2121213	σ_{12}
0000111	1212123	e
...	...	...

Table 9.1: C_{3v} correspondence between the binary labelled fundamental domain prime cycles $\bar{p}$ and the full 3-disk ternary labelled cycles p, together with the C_{3v} transformation that maps the end point of the $\bar{p}$ cycle into the irreducible segment of the p cycle, see sect. 19.2.2. Breaks in the ternary sequences mark repeats of the irreducible segment. The degeneracy of p cycle is $m_p = 6n_{\bar{p}}/n_p$. The shortest pair of the fundamental domain cycles related by time symmetry are the 6-cycles $\overline{001011}$ and $\overline{001101}$.

9.5 page 170

trajectory, a repeating binary symbols block corresponds either to the full periodic orbit or to an irreducible segment (examples are shown in fig. 9.5 and table 9.1). An irreducible segment corresponds to a periodic orbit in the fundamental domain. Table 9.1 lists some of the shortest binary periodic orbits, together with the corresponding full 3-disk symbol sequences and orbit symmetries. For a number of reasons that will be elucidated in chapter 19, life is much simpler in the fundamental domain than in the full system, so whenever possible our computations will be carried out in the fundamental domain.

Symbolic dynamics for N-disk game of pinball is so straightforward that one may altogether fail to see the connection between the topology of hyperbolic flows and their symbolic dynamics. This is brought out more clearly by the 1-d visualization of "stretch & fold" flows to which we turn now. Inspecting the fig. 9.3b we see that the relative ordering of regions with differing finite itineraries is a qualitative, topological property of the flow, so it makes sense to define a simple "canonical" representative partition which in a simple manner exhibits spatial ordering common to an entire class of topologically similar nonlinear flows.

in depth: chapter 19, p. 365

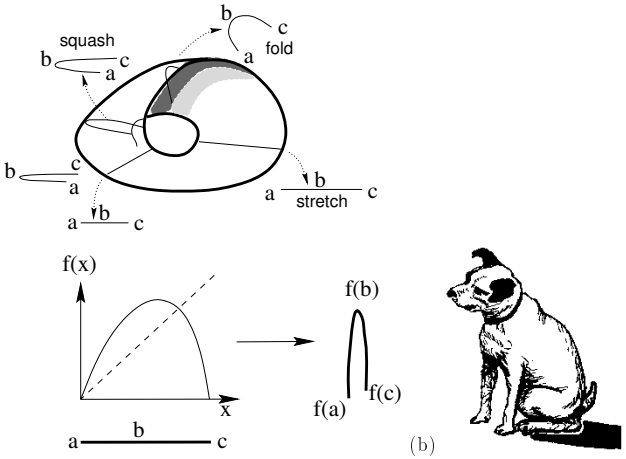

Figure 9.6: (a) A recurrent flow that stretches and folds. (b) The "stretch & fold" return map on the Poincaré section.

9.2 Stretch and fold

Suppose concentrations of certain chemical reactants worry you, or the variations in the Chicago temperature, humidity, pressure and winds affect your mood. All such properties vary within some fixed range, and so do their rates of change. Even if we are studying an operator system such as the 3-disk pinball game, we tend to be interested in a finite region around the disks and ignore the escapees. So a typical dynamical system that we care about is *bounded*. If the price for keeping going is high - for example, we try to stir up some tar, and observe it come to a dead stop the moment we cease our labors - the dynamics tends to settle into a simple limiting state. However, as the resistance to change decreases - the tar is heated up and we are more vigorous in our stirring - the dynamics becomes unstable. We have already quantified this instability in sect. 4.1 - for now, suffice it to say that a flow is *locally unstable* if nearby trajectories separate exponentially with time.

If a flow is locally unstable but globally bounded, any open ball of initial points will be stretched out and then folded back.

9.3 Going global: Stable/unstable manifolds

In sects. 7.1 and 9.1 we introduced the concept of partitioning the phase space, in any way you please. Here we show that the dynamics itself generates a natural partition.

In sect. 4.5 we established that stability eigenvalues of periodic orbits are invariants of a given flow. The invariance of stabilities of a periodic orbit is a local property of the flow. Now we show that every periodic orbit carries with it stable and unstable manifolds which provide a topologically invariant *global* foliation of the phase space.

A neighborhood of a trajectory deforms as it is transported by the flow. In the linear approximation, the matrix of variations A describes this shearing of an infinitesimal neighborhood in an infinitesimal time step. The shearing after finite time is described by the Jacobian matrix $\mathbf{J}^t$. Its eigenvalues and eigendirections describe deformation of an initial infinitesimal sphere of neighboring trajectories into an ellipsoid time t later. Nearby trajectories separate exponentially along the unstable directions, approach each other along the stable directions, and maintain their distance along the marginal directions.

The fixed or periodic point x^* stability matrix $\mathbf{J}_p(x^*)$ eigenvectors (4.42) describe the flow into or out of the fixed point only infinitesimally close to the fixed point. The global continuations of the local stable, unstable eigendirections are called the *stable*, respectively *unstable manifolds*. They consist of all points which march into the fixed point forward, respectively backward in time

$$\begin{aligned} W^s &= \left\{x \in \mathcal{M} : f^t(x) - x^* \to 0 \text{ as } t \to \infty\right\} \\ W^u &= \left\{x \in \mathcal{M} : f^{-t}(x) - x^* \to 0 \text{ as } t \to \infty\right\} . \end{aligned} \tag{9.8}$$

The stable/unstable manifolds of a flow are rather hard to visualize, so as long as we are not worried about a global property such as the number of times they wind around a periodic trajectory before completing a parcourse, we might just as well look at their Poincaré section return maps. Stable, unstable manifolds for maps are defined by

$$\begin{aligned} W^s &= \{x \in \mathcal{P} : f^n(x) - x^* \to 0 \text{ as } n \to \infty\} \\ W^u &= \left\{x \in \mathcal{P} : f^{-n}(x) - x^* \to 0 \text{ as } n \to \infty\right\} . \end{aligned} \tag{9.9}$$

For $n \to \infty$ any finite segment of W^s, respectively W^u converges to the linearized map eigenvector $\mathbf{e}^{(e)}$, respectively $\mathbf{e}^{(c)}$. In this sense each eigenvector defines a (curvilinear) axis of the stable, respectively unstable manifold. Conversely, we can use an arbitrarily small segment of a fixed point

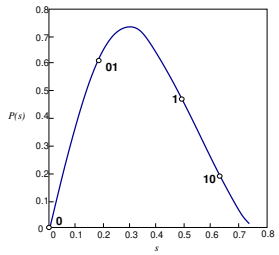

Figure 9.7: The Poincaré return map of the Kuramoto-Sivashinsky system (2.17) fig. 3.3, from the unstable manifold of the $\overline{1}$ fixed point to the (neighborhood of) the unstable manifold. Also indicated are the periodic points $\overline{0}$ and $\overline{01}$.

eigenvector to construct a finite segment of the associated manifold: The stable (unstable) manifold of the central hyperbolic fixed point (x_1, x_1) can be constructed numerically by starting with a small interval along the local stable (unstable) eigendirection, and iterating the interval n steps backwards (forwards).

Both in the example of the Rössler flow and of the Kuramoto-Sivashinsky system we have learned that the attractor is very thin, but otherwise the return maps that we found were disquieting – neither fig. 3.2 nor fig. 3.3 appeared to be one-to-one maps. This apparent loss of invertibility is an artifact of projection of higher-dimensional return maps onto lower-dimensional subspaces. As the choice of lower-dimensional subspace was entirely arbitrary, the resulting snapshots of return maps look rather arbitrary, too. Other projections might look even less suggestive. Such observations beg a question: Does there exist a "natural", intrinsically optimal coordinate system in which we should plot of a return map?

9.4 Temporal ordering: itineraries

In this section we learn how to *name* and *count* periodic orbits for the simplest, and nevertheless very instructive case, for 1-d maps of an interval.

Our next task is to relate the spatial ordering of phase-space points to their temporal itineraries. The easiest point of departure is to start out by working out this relation for the symbolic dynamics of 1-dimensional mappings. As it appears impossible to present this material without getting bogged down in a sea of 0's, 1's and subscripted symbols, let us state the main result at the outset: the admissibility criterion stated in sect. 9.5 eliminates *all* itineraries that cannot occur for a given unimodal map.

Suppose that the compression of the folded interval in fig. 9.6 is so fierce that we can neglect the thickness of the attractor. For example, the Rössler flow (2.11) is volume contracting, and an interval transverse to the attractor

is stretched, folded and pressed back into a nearly 1-dimensional interval, typically compressed transversally by a factor of $\approx 10^{13}$ in one Poincaré section return. In such cases it makes sense to approximate the return map of a "stretch & fold" flow by a 1-dimensional map. Simplest mapping of this type is *unimodal*; interval is stretched and folded only once, with at most two points mapping into a point in the new refolded interval. A *unimodal* map $f(x)$ is a 1-d function $\mathbb{R} \to \mathbb{R}$ defined on an interval $\mathcal{M}$ with a monotonically increasing (or decreasing) branch, a critical point or interval x_c for which $f(x_c)$ attains the maximum (minimum) value, followed by a monotonically decreasing (increasing) branch. The name is uninspiring - it refers to any one-humped map of interval into itself.

Example 9.2 Tent map. *The simplest examples of unimodal maps are the* complete tent map *fig. 9.8(a),*

$$f(\gamma) = 1 - 2|\gamma - 1/2|\,, \tag{9.10}$$

and the quadratic map (sometimes also called the logistic map)

$$x_{t+1} = 1 - a x_t^2\,, \tag{9.11}$$

with the one critical point at $x_c = 0$. Another example is the repelling unimodal map of fig. 9.8b. We refer to (9.10) as the "complete" tent map because its symbolic dynamics is a complete binary dynamics.

Such dynamical systems are irreversible (the inverse of f is double-valued), but, they may nevertheless serve as effective descriptions of hyperbolic flows.

For the unimodal maps of fig. 9.8 a Markov partition of the unit interval $\mathcal{M}$ is given by the two intervals $\{\mathcal{M}_0, \mathcal{M}_1\}$. The symbolic dynamics is complete binary: as both $f(\mathcal{M}_0)$ and $f(\mathcal{M}_1)$ fully cover $\mathcal{M}_0$ and $\mathcal{M}_1$, the corresponding transition matrix is a $[2\times2]$ matrix with all entries equal to 1, as in (9.3). The *critical value* denotes either the maximum or the minimum value of $f(x)$ on the defining interval; we assume here that it is a maximum, $f(x_c) \geq f(x)$ for all $x \in \mathcal{M}$. The critical value $f(x_c)$ belongs neither to the left nor to the right partition $\mathcal{M}_i$, and is denoted by its own symbol $s = C$.

The trajectory $x_1, x_2, x_3, \ldots$ of the initial point x_0 is given by the iteration $x_{n+1} = f(x_n)$. Iterating f and checking whether the point lands to the left or to the right of x_c generates a *temporally* ordered topological itinerary (9.16) for a given trajectory,

$$s_n = \begin{cases} 1 & \text{if } x_n > x_c \\ 0 & \text{if } x_n < x_c \end{cases}\,. \tag{9.12}$$

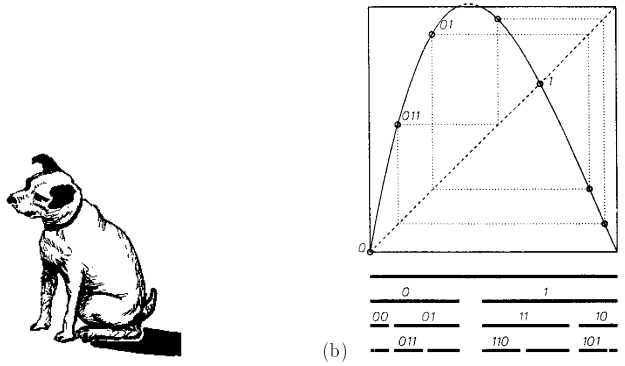

Figure 9.8: (a) The complete tent map together with intervals that follow the indicated itinerary for n steps. (b) A unimodal repeller with the remaining intervals after 1, 2 and 3 iterations. Intervals marked $s_1 s_2 \cdots s_n$ are unions of all points that do not escape in n iterations, and follow the itinerary $S^+ = s_1 s_2 \cdots s_n$. Note that the spatial ordering does not respect the binary ordering; for example $x_{00} < x_{01} < x_{11} < x_{10}$. Also indicated: the fixed points x_0, x_1, the 2-cycle $\overline{01}$, and the 3-cycle $\overline{011}$.

We shall refer to $S^+(x_0) = .s_1 s_2 s_3 \cdots$ as the future itinerary. Our next task is answer the reverse problem: given an itinerary, what is the corresponding *spatial* ordering of points that belong to a given trajectory?

As binary type symbolic dynamics pops up frequently, we list the shortest binary prime cycles in table 9.2.

9.3
page 169

9.5 Spatial ordering

The tent map (9.10) consists of two straight segments joined at $x = 1/2$. The symbol s_n defined in (9.12) equals 0 if the function increases, and 1 if the function decreases. The piecewise linearity of the map makes it possible to analytically determine an initial point given its itinerary, a property that we now use to define a topological coordinatization common to all unimodal maps.

Here we have to face the fundamental problems of combinatorics and symbolic dynamics: combinatorics cannot be taught. The best one can do is to state the answer, and then hope that you will figure it out by yourself. The tent map point $\gamma(S^+)$ with future itinerary S^+ is given by converting

n_p	p
1	0
	1
2	01
3	001
	011
4	0001
	0011
	0111
5	00001
	00011
	00101
	00111
	01011
	01111
6	000001
	000011
	000101
	000111
	001011
	001101
	001111
	010111
	011111
7	0000001
	0000011
	0000101

n_p	p
7	0001001
	0000111
	0001011
	0001101
	0010011
	0010101
	0001111
	0010111
	0011011
	0011101
	0101011
	0011111
	0101111
	0110111
	0111111
8	00000001
	00000011
	00000101
	00001001
	00000111
	00001011
	00001101
	00010011
	00010101
	00011001
	00100101

n_p	p
8	00001111
	00010111
	00011011
	00011101
	00100111
	00101011
	00101101
	00110101
	00011111
	00101111
	00110111
	00111011
	00111101
	01010111
	01011011
	00111111
	01011111
	01101111
	01111111
9	000000001
	000000011
	000000101
	000001001
	000010001
	000000111
	000001011

n_p	p
9	000001101
	000010011
	000010101
	000011001
	000100011
	000100101
	000101001
	000001111
	000010111
	000011011
	000011101
	000100111
	000101011
	000101101
	000110011
	000110101
	000111001
	001001011
	001001101
	001010011
	001010101
	000011111
	000101111
	000110111
	000111011
	000111101

n_p	p
9	001001111
	001010111
	001011011
	001011101
	001100111
	001101011
	001101101
	001110101
	010101011
	000111111
	001011111
	001101111
	001110111
	001111011
	001111101
	010101111
	010110111
	010111011
	001111111
	010111111
	011011111
	011101111
	011111111

Table 9.2: Prime cycles for the binary symbolic dynamics up to length 9.

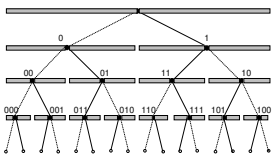

Figure 9.9: Alternating binary tree relates the itinerary labelling of the unimodal map fig. 9.8 intervals to their spatial ordering. Dotted line stands for 0, full line for 1; the binary sub-tree whose root is a full line (symbol 1) reverses the orientation, due to the orientation reversing fold in figs. 9.8 and 9.6.

the sequence of s_n's into a binary number by the following algorithm:

$$\begin{aligned} w_{n+1} &= \begin{cases} w_n & \text{if } s_n = 0 \\ 1 - w_n & \text{if } s_n = 1 \end{cases}, \qquad w_1 = s_1 \\ \gamma(S^+) &= 0.w_1 w_2 w_3 \ldots = \sum_{n=1}^{\infty} w_n / 2^n . \end{aligned} \tag{9.13}$$

This follows by inspection from the binary tree of fig. 9.9. For example, γ whose itinerary is $S^+ = 0110000\cdots$ is given by the binary number $\gamma = .010000\cdots$. Conversely, the itinerary of $\gamma = .01$ is $s_1 = 0$, $f(\gamma) = .1 \to s_2 = 1$, $f^2(\gamma) = f(.1) = 1 \to s_3 = 1$, etc..

9.6 page 170

We shall refer to $\gamma(S^+)$ as the *(future) topological coordinate*. w_t's are nothing more than digits in the binary expansion of the starting point γ for the complete tent map (9.10). In the left half-interval the map $f(x)$ acts by multiplication by 2, while in the right half-interval the map acts as a flip as well as multiplication by 2, reversing the ordering, and generating in the process the sequence of s_n's from the binary digits w_n.

The mapping $x_0 \to S^+(x_0) \to \gamma_0 = \gamma(S^+)$ is a *topological conjugacy* which maps the trajectory of an initial point x_0 under iteration of a given unimodal map to that initial point γ for which the trajectory of the "canonical" unimodal map (9.10) has the same itinerary. The virtue of this conjugacy is that it *preserves the ordering* for any unimodal map in the sense that if $\overline{x} > x$, then $\overline{\gamma} > \gamma$.

9.8 page 170

10.1 page 194

9.6 Topological dynamics

9.6.1 Finite memory

In the complete N-ary symbolic dynamics case (see example (9.3)) the choice of the next symbol requires no memory of the previous ones. However, any further refinement of the partition requires finite memory.

10.4 page 195

10.1 page 194

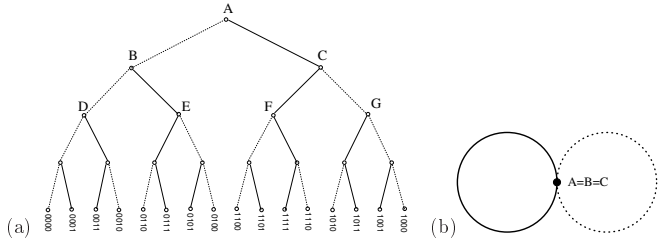

Figure 9.10: (a) The self-similarity of the complete binary symbolic dynamics represented by a binary tree (b) identification of nodes $B = A$, $C = A$ leads to the finite 1-node, 2-links Markov graph. All admissible itineraries are generated as walks on this finite Markov graph.

For example, for the binary labelled repeller with complete binary symbolic dynamics, we might chose to partition the phase space into four regions $\{\mathcal{M}_{00}, \mathcal{M}_{01}, \mathcal{M}_{10}, \mathcal{M}_{11}\}$, a 1-step refinement of the initial partition $\{\mathcal{M}_0, \mathcal{M}_1\}$. Such partitions are drawn in fig. 9.4, as well as fig. 1.8. Topologically f acts as a left shift, and its action on the rectangle [.01] is to move the decimal point to the right, to [0.1], forget the past, [.1], and land in either of the two rectangles $\{[.10], [.11]\}$. Filling in the matrix elements for the other three initial states we obtain the 1-step memory transition matrix acting on the 4-state vector

$$\phi' = T\phi = \begin{pmatrix} T_{00,00} & 0 & T_{00,10} & 0 \\ T_{01,00} & 0 & T_{01,10} & 0 \\ 0 & T_{10,01} & 0 & T_{10,11} \\ 0 & T_{11,01} & 0 & T_{11,11} \end{pmatrix} \begin{pmatrix} \phi_{00} \\ \phi_{01} \\ \phi_{10} \\ \phi_{11} \end{pmatrix} . \tag{9.14}$$

By the same token, for M-step memory the only nonvanishing matrix elements are of the form $T_{s_1 s_2 \ldots s_{M+1}, s_0 s_1 \ldots s_M}$, $s_{M+1} \in \{0, 1\}$. This is a sparse matrix, as the only non vanishing entries in the $m = s_0 s_1 \ldots s_M$ column of T_{dm} are in the rows $d = s_1 \ldots s_M 0$ and $d = s_1 \ldots s_M 1$. If we increase the number of steps remembered, the transition matrix grows big quickly, as the N-ary dynamics with M-step memory requires an $[N^{M+1} \times N^{M+1}]$ matrix. Since the matrix is very sparse, it pays to find a compact representation for T. Such representation is afforded by Markov graphs, which are not only compact, but also give us an intuitive picture of the topological dynamics.

Construction of a good Markov graph is, like combinatorics, unexplainable. The only way to learn is by some diagrammatic gymnastics, so we work our way through a sequence of exercises in lieu of plethora of baffling definitions.

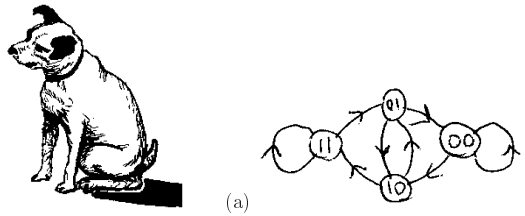

Figure 9.11: (a) The 2-step memory Markov graph, links version obtained by identifying nodes $A = D = E = F = G$ in fig. 9.10(a). Links of this graph correspond to the matrix entries in the transition matrix (9.14). (b) the 2-step memory Markov graph, node version.

To start with, what do finite graphs have to do with infinitely long trajectories? To understand the main idea, let us construct a graph that enumerates all possible iteneraries for the case of complete binary symbolic dynamics.

Mark a dot "." on a piece of paper. Draw two short lines out of the dot, end each with a dot. The full line will signify that the first symbol in an itinerary is "1", and the dotted line will signifying "0". Repeat the procedure for each of the two new dots, and then for the four dots, and so on. The result is the binary tree of fig. 9.10(a). Starting at the top node, the tree enumerates exhaustively all distinct finite itineraries

$$\{0,1\},\{00,01,10,11\},\{000,001,010,\cdots\},\cdots .$$

The $M = 4$ nodes in fig. 9.10(a) correspond to the 16 distinct binary strings of length 4, and so on. By habit we have drawn the tree as the alternating binary tree of fig. 9.9, but that has no significance as far as enumeration of itineraries is concerned - an ordinary binary tree would serve just as well.

The trouble with an infinite tree is that it does not fit on a piece of paper. On the other hand, we are not doing much - at each node we are turning either left or right. Hence all nodes are equivalent, and can be identified. To say it in other words, the tree is self-similar; the trees originating in nodes B and C are themselves copies of the entire tree. The result of identifying $B = A$, $C = A$ is a single node, 2-link Markov graph of fig. 9.10(b): any itinerary generated by the binary tree fig. 9.10(a), no matter how long, corresponds to a walk on this graph.

This is the most compact encoding of the complete binary symbolic dynamics. Any number of more complicated Markov graphs can do the job as well, and might be sometimes preferable. For example, identifying the

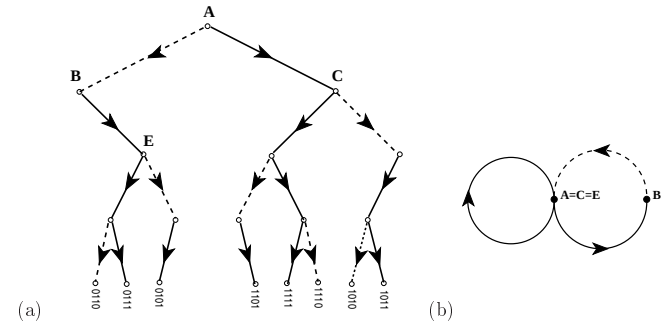

Figure 9.12: (a) The self-similarity of the _00_ pruned binary tree: trees originating from nodes C and E are the same as the entire tree. (b) Identification of nodes $A = C = E$ leads to the finite 2-node, 3-links Markov graph; as 0 is always followed by 1, the walks on this graph generate only the admissible itineraries.

trees originating in D, E, F and G with the entire tree leads to the 2-step memory Markov graph of fig. 9.11a. The corresponding transition matrix is given by (9.14).

fast track:
chapter 10, p. 171

9.7 Symbolic dynamics, basic notions

In this section we collect the basic notions and definitions of symbolic dynamics. The reader might prefer to skim through this material on first reading, return to it later as the need arises.

Shifts.

We associate with every initial point $x_0 \in \mathcal{M}$ the *future itinerary*, a sequence of symbols $S^+(x_0) = s_1 s_2 s_3 \cdots$ which indicates the order in which the regions are visited. If the trajectory $x_1, x_2, x_3, \ldots$ of the initial point x_0 is generated by

$$x_{n+1} = f(x_n)\,, \tag{9.15}$$

then the itinerary is given by the symbol sequence

$$s_n = s \qquad \text{if} \qquad x_n \in \mathcal{M}_s \,. \tag{9.16}$$

Similarly, the *past itinerary* $S^-(x_0) = \cdots s_{-2}s_{-1}s_0$ describes the history of x_0, the order in which the regions were visited before arriving to the point x_0. To each point x_0 in the dynamical space we thus associate a bi-infinite itinerary

$$S(x_0) = (s_k)_{k\in\mathbb{Z}} = S^-.S^+ = \cdots s_{-2}s_{-1}s_0.s_1s_2s_3\cdots \,. \tag{9.17}$$

The itinerary will be finite for a scattering trajectory, entering and then escaping $\mathcal{M}$ after a finite time, infinite for a trapped trajectory, and infinitely repeating for a periodic trajectory.

The set of all bi-infinite itineraries that can be formed from the letters of the alphabet $\mathcal{A}$ is called the *full shift*

$$\mathcal{A}^{\mathbb{Z}} = \{(s_k)_{k\in\mathbb{Z}} : s_k \in \mathcal{A} \text{ for all k } \in \mathbb{Z}\} \,. \tag{9.18}$$

The jargon is not thrilling, but this is how professional dynamicists talk to each other. We will stick to plain English to the extent possible.

We refer to this set of all conceivable itineraries as the *covering* symbolic dynamics. The name *shift* is descriptive of the way the dynamics acts on these sequences. As is clear from the definition (9.16), a forward iteration $x \to x' = f(x)$ shifts the entire itinerary to the left through the "decimal point". This operation, denoted by the shift operator σ,

$$\sigma(\cdots s_{-2}s_{-1}s_0.s_1s_2s_3\cdots) = \cdots s_{-2}s_{-1}s_0s_1.s_2s_3\cdots \,, \tag{9.19}$$

demoting the current partition label s_1 from the future S^+ to the "has been" itinerary S^-. The inverse shift σ^{-1} shifts the entire itinerary one step to the right.

A finite sequence $b = s_k s_{k+1}\cdots s_{k+n_b-1}$ of symbols from $\mathcal{A}$ is called a *block* of length n_b. A phase space trajectory is *periodic* if it returns to its initial point after a finite time; in the shift space the trajectory is periodic if its itinerary is an infinitely repeating block p^∞. We shall refer to the set of periodic points that belong to a given periodic orbit as a *cycle*

$$p = \overline{s_1 s_2 \cdots s_{n_p}} = \{x_{s_1 s_2\cdots s_{n_p}}, x_{s_2\cdots s_{n_p}s_1}, \cdots, x_{s_{n_p}s_1\cdots s_{n_p-1}}\} \,. \tag{9.20}$$

By its definition, a cycle is invariant under cyclic permutations of the symbols in the repeating block. A bar over a finite block of symbols denotes a periodic itinerary with infinitely repeating basic block; we shall omit the bar whenever it is clear from the context that the trajectory is periodic. Each *cycle point* is labeled by the first n_p steps of its future itinerary. For example, the 2nd cycle point is labelled by

$$x_{s_2\cdots s_{n_p}s_1} = x_{\overline{s_2\cdots s_{n_p}s_1}.\overline{s_2\cdots s_{n_p}s_1}} \,.$$

A *prime* cycle p of length n_p is a single traversal of the orbit; its label is a block of n_p symbols that cannot be written as a repeat of a shorter block (in literature such cycle is sometimes called *prime*; we shall refer to it as "prime" throughout this text).

Partitions.

A partition is called *generating* if every infinite symbol sequence corresponds to a distinct point in the phase space. Finite Markov partition (9.4) is an example. Constructing a generating partition for a given system is a difficult problem. In examples to follow we shall concentrate on cases which allow finite partitions, but in practice almost any generating partition of interest is infinite.

A mapping $f : \mathcal{M} \to \mathcal{M}$ together with a partition $\mathcal{A}$ induces *topological dynamics* (Σ, σ), where the *subshift*

$$\Sigma = \{(s_k)_{k\in\mathbb{Z}}\} \,, \tag{9.21}$$

is the set of all *admissible* infinite itineraries, and $\sigma : \Sigma \to \Sigma$ is the shift operator (9.19). The designation "subshift" comes form the fact that $\Sigma \subset \mathcal{A}^{\mathbb{Z}}$ is the subset of the full shift (9.18). One of our principal tasks in developing symbolic dynamics of dynamical systems that occur in nature will be to determine Σ, the set of all bi-infinite itineraries S that are actually realized by the given dynamical system.

A partition too coarse, coarser than, for example, a Markov partition, would assign the same symbol sequence to distinct dynamical trajectories. To avoid that, we often find it convenient to work with partitions finer than strictly necessary. Ideally the dynamics in the refined partition assigns a unique infinite itinerary $\cdots s_{-2}s_{-1}s_0.s_1s_2s_3\cdots$ to each distinct trajectory, but there might exist full shift symbol sequences (9.18) which are not realized as trajectories; such sequences are called *inadmissible*, and we say that the symbolic dynamics is *pruned*. The word is suggested by "pruning" of branches corresponding to forbidden sequences for symbolic dynamics organized hierarchically into a tree structure, as explained in sect. 9.6.

Pruning.

If the dynamics is pruned, the alphabet must be supplemented by a *grammar*, a set of pruning rules. After the inadmissible sequences have been pruned, it is often convenient to parse the symbolic strings into words of variable length - this is called *coding*. Suppose that the grammar can be stated as a finite number of pruning rules, each forbidding a block of finite length,

$$\mathcal{G} = \{b_1, b_2, \cdots b_k\} \ , \tag{9.22}$$

where a *pruning block* b is a sequence of symbols $b = s_1 s_2 \cdots s_{n_b}$, $s \in \mathcal{A}$, of finite length n_b. In this case we can always construct a finite Markov partition (9.4) by replacing finite length words of the original partition by letters of a new alphabet. In particular, if the longest forbidden block is of length $M+1$, we say that the symbolic dynamics is a shift of finite type with M-step memory. In that case we can *recode* the symbolic dynamics in terms of a new alphabet, with each new letter given by an admissible block of at most length M. In the new alphabet the grammar rules are implemented by setting $T_{ij} = 0$ in (9.3) for forbidden transitions.

A topological dynamical system (Σ, σ) for which all admissible itineraries are generated by a finite transition matrix

$$\Sigma = \left\{ (s_k)_{k\in\mathbb{Z}} \ : T_{s_k s_{k+1}} = 1 \quad \text{for all } k \right\} \tag{9.23}$$

is called a subshift of *finite type*. Such systems are particularly easy to handle; the topology can be converted into symbolic dynamics by representing the transition matrix by a finite directed *Markov graph*, a convenient visualization of topological dynamics.

Markov graphs.

A Markov graph describes compactly the ways in which the phase-space regions map into each other, accounts for finite memory effects in dynamics, and generates the totality of admissible trajectories as the set of all possible walks along its links.

A Markov graph consists of a set of *nodes* (or *vertices*, or *states*), one for each state in the alphabet $\mathcal{A} = \{A, B, C, \cdots, Z\}$, connected by a set of directed *links* (*edges*, *arcs*). Node i is connected by a directed link to node j whenever the transition matrix element (9.2) takes value $T_{ij} = 1$.

(a) $T = \begin{pmatrix} 1 & 1 \\ 1 & 0 \end{pmatrix}$ (b)

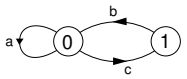

Figure 9.13: (a) The transition matrix for a simple subshift on two-state partition $\mathcal{A} = \{0, 1\}$, with grammar $\mathcal{G}$ given by a single pruning block $b = 11$ (consecutive repeat of symbol 1 is inadmissible): the state $\mathcal{M}_0$ maps both onto $\mathcal{M}_0$ and $\mathcal{M}_1$, but the state $\mathcal{M}_1$ maps only onto $\mathcal{M}_0$. (b) The corresponding finite 2-node, 3-links Markov graph, with nodes coding the symbols. All admissible itineraries are generated as walks on this finite Markov graph.

There might be a set of links connecting two nodes, or links that originate and terminate on the same node. Two graphs are isomorphic if one can be obtained from the other by relabelling links and nodes; for us they are one and the same graph. As we are interested in recurrent dynamics, we restrict our attention to *irreducible* or *strongly connected* graphs, that is graphs for which there is a path from any node to any other node.

The simplest example is given in fig. 9.13.

Résumé

Symbolic dynamics is the coarsest example of coarse graining, the way irreversibility enters chaotic dynamics. The exact trajectory is deterministic, and given an initial point we know (in principle) both its past and its future - its memory is infinite. In contrast, the partitioned phase space is described by the quientessentially probabilistic tools, such as the finite memory Markov graphs.

In chapters 11 and 12 we will establish that spectra of evolution operators can be extracted from periodic orbit sums:

$$\sum (\text{spectral eigenvalues}) \ = \ \sum (\text{periodic orbits}) \ .$$

In order to implement this theory we need to know what periodic orbits can exist, and the symbolic dynamics developed above is an invaluable tool toward this end.

Importance of symbolic dynamics is sometime grossly unappreciated; the crucial ingredient for nice analyticity properties of zeta functions is existence of finite grammar (coupled with uniform hyperbolicity).

References

[9.1] B.P. Kitchens, Symbolic dynamics: one-sided, two-sided, and countable state Markov shifts (Springer, Berlin 1998).

[9.2] D.A. Lind and B. Marcus, *An introduction to symbolic dynamics and coding* (Cambridge Univ. Press, Cambridge 1995).

[9.3] Fa-geng Xie and Bai-lin Hao, "Counting the number of periods in one-dimensional maps with multiple critical points", *Physica A*, **202**, 237 (1994).

[9.4] Hao Bai-Lin, *Elementary symbolic dynamics and chaos in dissipative systems* (World Scientific, Singapore, 1989).

[9.5] R.L. Devaney, *A First Course in Chaotic Dynamical Systems* (Addison-Wesley, Reading MA, 1992).

[9.6] R.L. Devaney, *An Introduction to Chaotic Dynamical Systems* (Addison-Wesley, Reading MA, 1987).

[9.7] J. Guckenheimer and P. Holmes, *Non-linear Oscillations, Dynamical Systems and Bifurcations of Vector Fields* (Springer, New York, 1986).

[9.8] A. Salomaa, *Formal Languages* (Academic Press, San Diego, 1973).

[9.9] J.E. Hopcroft and J.D. Ullman, *Introduction to Automata Theory, Languages, and Computation* (Addison-Wesley, Reading MA, 1979).

[9.10] D.M. Cvetković, M. Doob and H. Sachs, *Spectra of Graphs* (Academic Press, New York, 1980).

[9.11] T. Bedford, M.S. Keane and C. Series, eds., *Ergodic Theory, Symbolic Dynamics and Hyperbolic Spaces* (Oxford University Press, Oxford, 1991).

[9.12] M.S. Keane, *Ergodic theory and subshifts of finite type*, in ref. [9.11].

[9.13] P.J. Myrberg, *Ann. Acad. Sc. Fenn., Ser. A,* **256**, 1 (1958); **259**, 1 (1958).

[9.14] N. Metropolis, M.L. Stein and P.R. Stein, *On Finite Limit Sets for Transformations on the Unit Interval*, *J. Comb. Theo.* **A15**, 25 (1973).

[9.15] A.N. Sarkovskii, *Ukrainian Math. J.* **16**, 61 (1964).

[9.16] J. Milnor and W. Thurston, *"On iterated maps of the interval"*, in A. Dold and B. Eckmann, eds., *Dynamical Systems, Proceedings, U. of Maryland 1986-87*, *Lec. Notes in Math.* **1342,** 465 (Springer, Berlin, 1988).

[9.17] W. Thurston, *"On the geometry and dynamics of diffeomorphisms of surfaces"*, *Bull. Amer. Math. Soc. (N.S.)* **19**, 417 (1988).

[9.18] P. Collet and J.P. Eckmann, *Iterated Maps on the Interval as Dynamical Systems* (Birkhauser, Boston, 1980).

[9.19] V. Baladi and D. Ruelle, *"An extension of the theorem of Milnor and Thurston on the zeta functions of interval maps"*, *Ergodic Theory Dynamical Systems* **14**, 621 (1994).

[9.20] V. Baladi, *"Infinite kneading matrices and weighted zeta functions of interval maps"*, *J. Functional Analysis* **128**, 226 (1995).

[9.21] D. Ruelle, *"Sharp determinants for smooth interval maps"*, Proceedings of Montevideo Conference 1995, IHES preprint (March 1995).

[9.22] V. Baladi and D. Ruelle, *"Sharp determinants"*, *Invent. Math.* **123**, 553 (1996).

[9.23] P. Cvitanović, G.H. Gunaratne and I. Procaccia, *Phys. Rev.* **A 38**, 1503 (1988).

[9.24] G. D'Alessandro, P. Grassberger, S. Isola and A. Politi, "On the topology of the Hénon Map", *J. Phys.* **A 23**, 5285 (1990).

[9.25] G. D'Alessandro, S. Isola and A. Politi, "Geometric properties of the pruning front", *Prog. Theor. Phys.* **86**, 1149 (1991).

[9.26] Y. Ishii, "Towards the kneading theory for Lozi attractors. I. Critical sets and pruning fronts", Kyoto Univ. Math. Dept. preprint (Feb. 1994).

[9.27] Y. Ishii, "Towards a kneading theory for Lozi mappings. II. A solution of the pruning front conjecture and the first tangency problem", *Nonlinearity* (1997), to appear.

[9.28] A. de Carvalho, Ph.D. thesis, CUNY New York 1995; "Pruning fronts and the formation of horseshoes", preprint (1997).

[9.29] K.T. Hansen, *CHAOS* **2**, 71 (1992).

[9.30] K.T. Hansen, *Nonlinearity* **5**

[9.31] K.T. Hansen, *Nonlinearity* **5**

[9.32] K.T. Hansen, *Symbolic dynamics III, The stadium billiard*, to be submitted to *Nonlinearity*

[9.33] K.T. Hansen, *Symbolic dynamics IV; a unique partition of maps of Hénon type*, in preparation.

[9.34] E. Aurell, *"Convergence of dynamical zeta functions"*, *J. Stat. Phys.* **58**, 967 (1990).

[9.35] M. Benedicks and L. Carleson, *Ann. of Math.*, **122**, 1 (1985).

[9.36] P. Dahlqvist, *On the effect of pruning on the singularity structure of zeta functions*, J. Math. Phys. **38**, 4273 (1997).

[9.37] E. Hille, *Analytic function theory II* (Ginn and Co. 1959).

[9.38] P.H. Richter, H-J. Scholz and A. Wittek, "A Breathing Chaos", *Nonlinearity* **1**, 45 (1990).